

Full Length Research Paper

# Mineral and geochemical characterization of the weathering mantle derived from norites in Kekem (West Cameroon): evaluation of the related mineralization

Tematio Paul<sup>1</sup>, Kombou Nina Aurelie<sup>1</sup>, Kengni Lucas<sup>1</sup>, Nguetnkam Jean Pierre<sup>2</sup>, and Kamgang-Kabeyene Véronique<sup>3</sup>

<sup>1</sup>University of Dschang, Faculty of Science, Dschang, Cameroon

<sup>2</sup>University of Ngaoundere, Faculty of Science, Ngaoundere, Cameroon

<sup>3</sup>University of Yaoundé I, ENS, Yaoundé, Cameroon

Accepted 15 October, 2012

In West Cameroon, the Kekem weathering mantle exhibited a shallow weathered soil pedon with seven differentiated soil phases. The secondary minerals consist of akaganéite, sepiolite, berthierine and smectite. Phlogopite, feldspar and pyroxene, which are not completely weathered, remain present in specific soil phases. Silica (37.2 - 43.9%), aluminum (16.8 - 23.7%) and iron (9.9 - 15.9%) are the most abundant major elements. Calcium and sodium are almost completely leached, whereas potassium (4.2%) and magnesium contents (6.9%) increase with depth. The most abundant trace elements are Ba (3309.0 ppm), Cr (1133.0 ppm), V (638.0 ppm), Sr (428.1 ppm), Zr (238.0 ppm), Ni (227.9 ppm), Co (174.4 ppm), Zn (139.0 ppm) and Rb (102.7 ppm). Chromium with enrichment factor, EF: 9.1 - 48.1, Cu (EF: 3.0 - 4.9), Hf (EF: 1.9 - 3.5), V (EF: 1.4 - 4.0), Nb (EF: 0.9 - 3.0), Ta (EF: 0.8 - 3.7), Th (EF: 0.9 - 2.3), U (EF: 0.9 - 2.8) and W (EF: 0.6 - 1.8) are enriched in soil phases. The light rare earth elements (LREE) are the most abundant REE in soils, with  $\Sigma$ LREE ranging from 69.5 to 293.4 ppm. The REE in various soil phases are strongly fractionated from La to Dy, with important Eu anomaly.

**Keywords:** West Cameroon, Norites weathering mantle, Akaganéite, Sepiolite, Berthierine, Rare metals.

## INTRODUCTION

Norites are basic intrusive igneous rocks composed largely of calcium-rich plagioclase and hypersthene. Their weathering is commonly associated with rare metals and platinum group elements (PGE) mineralization. It is the case in the Bushveld complex in South Africa with platinum (Moyen, 2007 ; Lee, 1996 ), the Okiep Copper District in South Africa (Hamman *et al.*, 1996), the Stillwater complex in Montana (USA), the Sudbury Basin

complex in Ontario (Canada) which is the world's second largest nickel mining region (Ames and Farrow, 2007) and the Gombak norite in Bukit Gombak (Singapore) (Singh *et al.*, 2012).

Norites have been described by Kwékam (2005) in Kekem, a part of the Cameroon volcanic line (CVL) with various volcanic products and Neoproterozoic Pan-African basement (Kwékam *et al.*, 2010). They are basic intrusive rocks with high amounts of feldspars (40 to 50%) and pyroxenes (20 to 30%). Additionally, these rocks have 54 to 59% of SiO<sub>2</sub>, 4 to 14% of MgO, 5 to 7% of CaO, 3 to 5% of K<sub>2</sub>O, and relatively high contents of Ba (2831 ppm), Cr (1321 ppm) and Sr (1602 ppm). In Cameroon, no previous investigations have been carried out on the weathering mantles derived from norites. The only studies were on basic rocks (serpentinite)

\*Corresponding Author E-mail: [paul\\_tematio@yahoo.fr](mailto:paul_tematio@yahoo.fr)  
[paul\\_tematio@univ-dschang.com](mailto:paul_tematio@univ-dschang.com); Tel. (237) 94 32 04 84

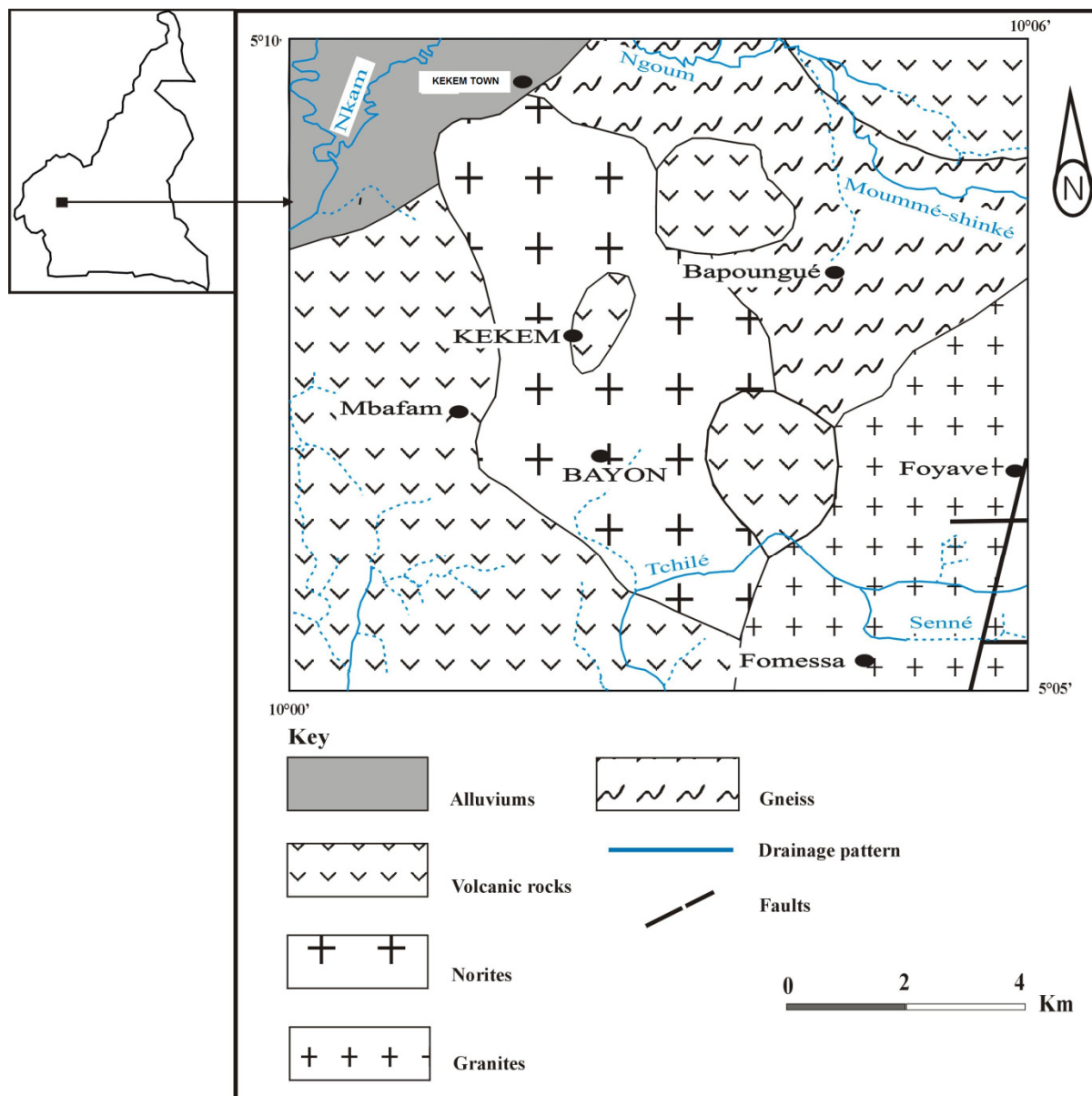


**Figure 1.** Geological map and location of the Kekem area

in the southern region of Cameroon (Ndjigui *et al.*, 2008; Yongue-Fouateu *et al.*, 2006; Yongue-Fouateu, 1995). These studies indicate that the weathering of serpentinite has led to accumulation of chlorite, smectite, talc, goethite, maghemite, hematite, kaolinite and gibbsite; that the highest concentrations of Ni, Co and Cr are in the saprolite; and that the concentration of U and Th increase upwards in the weathering mantle. This paper deals with a detailed exploration of the weathering mantle of Kekem norites in order to document and explain the origin of sepiolite, akaganéite and berthierine, and the occurrence of medium grade accumulation of rare metals in this area. This calls for

detailed investigation of soil phases in this weathering mantle that cover their macroscopic and microscopic organization, characterization of their minerals and mobilization and distribution of their chemical elements.

### Regional setting

The Kekem basic intrusive complex is located in the foot-slopes of the southern edge of the *Bamiléké plateau*, between latitudes 5°05' and 5°10' north, and longitudes 10°00' and 10°06' east (Figure 1). This area is under the

influence of the rain forest equatorial climate with more than 2000 mm of annual rainfall and about 23°C of mean annual temperature. Morphologically, it shows an undulating landscape of lowlands which corresponds to the east extension of the Mbô plain, a major graben of the Cameroon volcanic line (Déruelle *et al.*, 1991). This area also exhibits numerous mineral springs with whitish foams all around it, indicative of a highly confined alkaline environment.

From a geological point of view, the Kekem basic complex is a basic intrusion of about 10 km wide made up of norites and gabbros (Kwékam, 2005) (Figure 1). Norites are predominant with gabbros located mainly at the edge of the massif. These norites, mostly medium-grained, are made up of feldspars, pyroxenes and phlogopites (Kwékam *et al.*, *in press*). Ilmenite, Cr-rich magnetite, rutile, apatite and zircon are the main accessory minerals. Feldspars display large variation in composition and consist of plagioclase (40 to 50%) and alkali feldspar (<5%). Plagioclases range from labradorite to oligoclase, but oligoclase ( $An_{32-55}Ab_{44-66}$ ) and alkali-feldspar ( $Or_{32-87}Ab_{12-13}An_{0.3-7}$ ) are common. Pyroxenes are made up of diopsides (20 to 30%) and enstatites (20%). Diopside composition is less magnesian ( $Wo_{45-46}En_{38-39}Fs_{15-17}$ , with  $X_{Mg}$  equal to 0.72 - 0.76). Enstatite composition is close to  $Wo_{0-3}En_{60-75}Fs_{25-39}$ , with  $X_{Mg}$  equal to 0.61 - 0.75 and generally poor in Al ( $Al^{IV}$ : 0.0 - 0.014 p.f.u). Phlogopite, 10 to 20%, is relatively rich in magnesium, with  $X_{Mg}$  equal to 0.67 - 0.69. Chemically, the major element contents range from 54.2 to 58.7% for  $SiO_2$ , 6.1 to 9.2% for  $Fe_2O_3$  and 3.7 to 13.8% for MgO. The most abundant trace element is Ba (2831 ppm), followed by Cr (1321 ppm), Sr (1297 ppm), in association with Ni (345 ppm), Zr (275 ppm), V (190 ppm) and Rb (156 ppm). Lead (Pb) reaches an average of 22.1 ppm. Concentrations of the rare earth elements (REE) are very high compared to the bulk silicate earths (BSE) (Mc Donough and Sun, 1995), with enrichment rates (ER) varying from 3.4 for Yb to 81.3 for La (not shown). The light rare earth elements (LREE) have higher concentrations (ER: 22.4 to 81.3 times) than the heavy rare earth elements (HREE). The most abundant REE is Ce (101.6 ppm), followed by La (64.0 ppm), Nd (52.4 ppm), with smaller amounts of Pr (12.8 ppm), Gd (9.9 ppm), Sm (9.7 ppm) and Dy (8.2 ppm). Chondrite-normalized REE abundance in the Kekem norites (cf Figure 5 below) exhibits a typical pattern of the upper continental crust (McLennan, 1989) and also evidence REE enrichment accompanied by strong La to Dy fractionation.

## METHODS OF STUDY

The Kekem weathering mantle was exposed by hand dug wells cut through the soil to the unweathered parent rock.

Soil pedons were differentiated by soil horizons with various soil phases; a macroscopic description of these soil phases was made. After soil profiles excavation, soil samples were collected from the various soil phases (see Figure 2 below), air-dried and crushed into a fine powder prior to mineral and chemical analyses.

Mineral analysis was done using X-ray powder diffraction (XRD) on un-oriented powdered whole-samples. The XRD analysis were performed in the MIPROMALO laboratory (Cameroon) using a BRUKER type diffractometer with Cu-K $\alpha$  radiation,  $\lambda$ : 1.5418Å, with a scan mode between  $2\theta$ : 5 - 90°, with  $2\theta$  step of 0.002° and a scanning speed of 1°/min. Relative amounts of each mineral in the soil sample were obtained from the intensity of its principal basal reflection. For chemical analyses, the whole-samples of fine grained soil phases were sent to GeoLab (Ontario, Canada) for major, trace and rare earth elements determination and quantification. Chemical elements identification and quantification was performed by the X-ray fluorescence spectrometry method using a Philips XRFSPW1404 spectrometer. Mass contents are reported as percent of oxides (%) for major elements and part per million (ppm) for trace and rare earth elements.

In addition, three soil weathering indices were inferred from the major element data. They are: the chemical index of alteration ( $CIA = [Al_2O_3 / (Al_2O_3 + CaO^* + Na_2O)] \times 100$ , where  $CaO^*$  is the content of calcium oxide in fresh rock) (Nestbitt and Young, 1989), the molar ratio  $SiO_2/Al_2O_3$  (Ruxton, 1968) and the bases/ $R_2O_3$  ratio that equal to  $[(MgO + CaO + Na_2O + K_2O) / (Al_2O_3 + Fe_2O_3 + TiO_2)] \times 100$  (Birkeland, 1999). Chemical mass balance between soil phases were estimated from the calculations of enrichment/depletion factors determined using Ti as immobile element. Enrichment factor (EF) was estimated by the ratio between the content of an element in a soil phase and that of fresh rock according to the relation  $EF(X) = (X_i/R_i) / (X_s/R_s)$  (Rahn and Mc Cafrey, 1979), where  $X_i$  and  $R_i$  are the concentrations of the element of interest and that of a reference element (Ti) in a given soil phase and  $X_s$  and  $R_s$  are the concentrations of the same elements in fresh rock. The REE concentrations were normalized relative to CI Chondrite (Anders and Grevesse, 1989) to facilitate the comparison of the REE patterns between soil phases. The  $(La/Yb)_N$  ratios were calculated to indicate the degree of LREE to HREE fractionation, while the  $(La/Sm)_N$  measures the degree of LREE to MREE fractionation. Europium (Eu) anomalies were estimated by comparing the measured concentration of Eu with an expected concentration ( $Eu^*$ ) obtained by interpolation between the normalized values of Sm and Gd, as proposed by Taylor and McLennan (Taylor and McLennan, 1985).

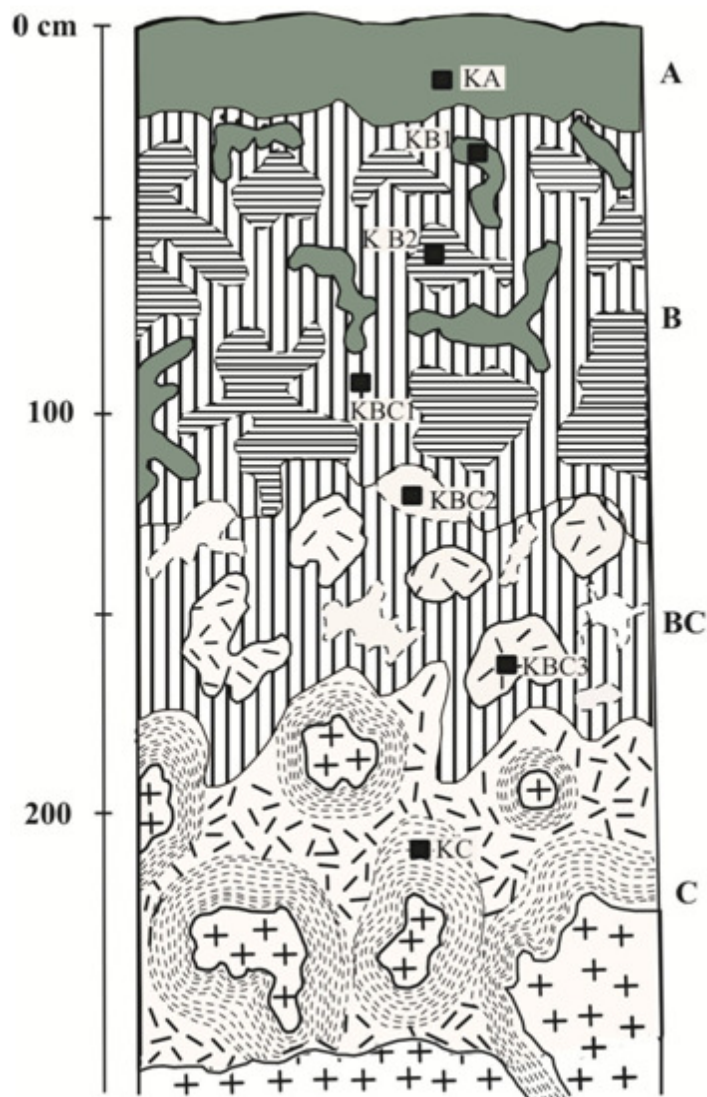


**Figure 2.** Macroscopic organization of the Kekem weathering mantle typical soil pedon and location of the sampling sites (*KC*, pink saprolite; *KBC3*, reddish brown saprolite; *KBC2*, whitish grey soil matrix; *KBC1*, yellow brown soil matrix; *KB2*, pale red soil matrix; *KB1*, dark grey soil matrix; *KA*, dark brown soil matrix)

## RESULTS

### Minerals association and characterization in various soil phases

Vertical organization of the typical soil pedon from this weathering mantle is illustrated in Figure 2.

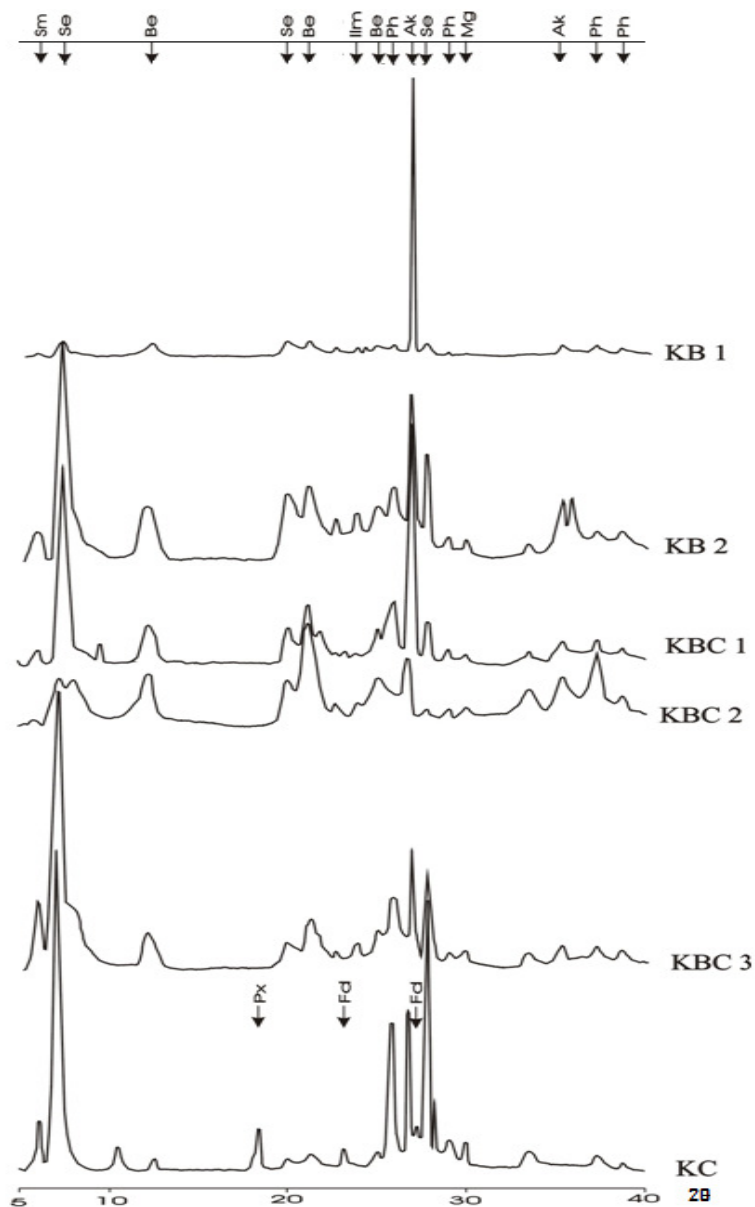
This weathering mantle exhibits a 2.5 m thick shallow weathered soil pedon with A, B, BC, and C soil horizons (Figure 2). The surface A horizon is 26 cm thick and has a dark brown (7.5 YR 3/4), clayey, fragile, crumbly and fine granular soil matrix (Table 1). Its transition to the underlying B horizon is distinct and regular. This

subsurface B horizon is 100 cm thick; is heterogeneous, with pale red (10 R 5/3), clayey, slightly cemented and undifferentiated soil matrix which forms centimetric domains embedded into yellow brown (7.5 YR 5/8) and clayey soil matrix with coarse sub-angular to polyhedral structure. Both soil matrices are cut off by wormlike cavities infilled with dark grey (5 YR 3/1), clayey, fragile and crumbly soil matrix with fine granular structure. The subsurface B horizon grades progressively downward to a 50 cm thick BC horizon which is also heterogeneous, with saprolite boulders and whitish grey domains embedded into the above yellow brown soil matrix. The saprolite boulders are strongly weathered, but still

**Table 1.** Minerals and their relative abundance in various soil phases

<i>Minerals</i>	<i>Horizon</i> <i>Soil phases</i>	<i>R</i>	<i>C</i> (176 - 250cm)		<i>BC</i> (126 - 176cm)		<i>B</i> (26 - 126cm)	
		<i>KR</i>	<i>KC</i>	<i>KBC3</i>	<i>KBC2</i>	<i>KBC1</i>	<i>KB2</i>	<i>KB1</i>
Akaganéite	relative amounts in %	-	18	16	25	40	21	75
Berthierine		-	3	9	38	8	14	8
Sepiolite		-	44	32	19	34	32	10
Smectite		-	8	16	-	3	4	-
Phlogopite		10-20	20	14	18	15	21	7
Feldspars		40-50	4	7	-	-	8	-
Pyroxenes		20-30	3	3	6	-	-	-

-: not detected

**Figure 3.** The X-ray diffraction patterns of the Kekem weathering mantle (*Sm*: smectite; *Se*: sepiolite; *Be*: berthierine; *Ph*: phlogopite; *Ak*: akaganéite; *Px*: pyroxene; *Fd*: feldspar)

preserve the medium-grainy structure of fresh norites. They comprise a reddish brown (10 R 3/2), silty sand and undifferentiated weathered material with abundant micrometric and polychromatic punctuations. The whitish grey domains are centimetric, whitish grey (10 YR 7/1) in color, clayey and very porous. The saprolite boulders of the BC horizon become bigger with depth and demarcate an almost continuous C horizon between 176 and 250cm. This lowermost C horizon has a pink (7.5 YR 7/4), silty sand, undifferentiated and strongly weathered material with original structure of preserved fresh norites, and partially weathered norites boulders. Fresh unweathered norites occur in the core of these boulders. Thus, macroscopically, the typical soil pedon of the Kekem weathering mantle has differentiated seven soil phases (Figure 2): the *dark brown soil matrix* sampled KA in the A horizon; the *dark grey (KB1)*, *pale red (KB2)* and *yellow brown (KBC1) soil matrices* in the B horizon; the *whitish grey (KBC2)* and *yellow brown soil matrices*, and the *reddish brown saprolite (KBC3)* in the BC horizon; and the *pink saprolite (KC)* in the C horizon.

Under the optical microscope, the seven soil phases exhibit six s-matrices: isalteritic, whitish grey, yellow brown, dark grey, pale red and dark brown s-matrices. The isalteritic s-matrix refers to the pink and the reddish brown saprolites. It is made up of both crystal-rich and clayey plasmas. The crystal-rich plasma is similar to more or less weathered crystals of feldspars. In the pink saprolite, it forms a continuous frame representing about 45% of the s-matrix. It falls below 10% in the reddish brown saprolite where it appears as centimetric and diffuse domains embedded into the clayey plasma. The clayey plasma is made up of brown red ferruginous matrix underlying contours and splittings of not completely weathered pyroxenes, or forming more or less homogeneous veil over the crystal-rich plasma. The whitish grey s-matrix refers to the whitish grey soil phase. It is porphyritic, with a whitish grey and argilasepic plasma that forms continuous matrix densely dissected by micro-cracks. The yellow brown s-matrix represents the yellow brown soil phase. It is also porphyritic, with both yellow brown and dark red plasmas. The yellow brown plasma, making up more than 55% of the s-matrix, is yellow and locally brown in color, clayey and argilasepic. It still contains relics of partially weathered phlogopites and crystal-rich plasma. The dark red plasma did not exceed 10% of the s-matrix. It shows an isotropic fabric and forms 2 to 5 mm wide diffuse micro-domains scattered into the yellow brown plasma. The pale red s-matrix refers to the pale red soil phase. It is porphyritic, with reddish brown and locally isotropic ferruginous plasma. The dark grey s-matrix corresponds to the dark grey soil phase. It is agglomeroplasmic, with grayish, continuous, more or less homogeneous and argilasepic clayey plasma. It still contains isotropic micro-domains and abundant packing voids. The dark brown s-matrix

represents the dark brown soil phase. It exhibits the same microscopic characteristics as the dark grey s-matrix. Thus, at a microscopic scale, the seven soil phases of the Kekem weathering mantle may have differentiated five s-matrices: *isalteritic*, *yellow brown*, *whitish grey*, *pale red* and *dark grey to dark brown s-matrices*.

### Minerals association and characterization of various soil phases

Minerals and their relative abundance in various soil phases are summarized in Table 1 and their X-ray diffraction patterns illustrated in Figure 3.

In this weathering mantle, all the soil phases have approximately the same secondary mineral composition, which consist of akaganéite, sepiolite, berthierine and smectite. Partially weathered primary minerals such as phlogopites, feldspars and pyroxenes are still present in some soil phases. Akaganéite (16 to 75% of minerals detected by X-ray) and sepiolite (10 to 44%) are the dominant weathering products. Akaganéite is easily recognized in the X-ray patterns by its basal reflection at 3.32 Å (Figure 3). It occurs in all the soil phases, with the highest values in the yellow brown and the dark grey soil matrices, respectively (40% and 75%) (Table 1). Sepiolite was identified in the X-ray patterns by its major peak around 12.02 Å (Figure 3). Its highest content is in the pink saprolite (44%). It reduces gradually upwards to 10% in the dark grey soil matrix at topsoil. Both the above weathering products are associated with important amounts of berthierine (3 to 38%) and phlogopite (7 to 21%), and relatively low contents of smectite (3 to 16%) (Table 1). Berthierine also occurs in all the soil phases, with its highest contents in the whitish grey soil matrix of the BC horizon (38%). It exhibits distinct basal reflections at 7.12 Å, 3.54 Å and 2.54 Å, respectively (Figure 3). Smectite also occur in various soil phases, except in the whitish grey and the dark grey soil matrices. In the X-ray diffraction patterns, this mineral displays distinct reflection at 14.15 - 14.25 Å. Phlogopite, a magnesium-rich biotite, is the unique partially weathered primary mineral remaining in all the soil phases. It ranges from 7 to 21% of the minerals detected by X-ray (Table 1). In the X-ray diffraction patterns, it shows a basal reflection between 9.9Å and 10.1Å. Pyroxene, another partially weathered primary mineral which represents about 3 to 6% of the minerals, is only reported at soil depths in the pink and the reddish brown saprolites. Feldspar, which constitutes about 4 to 8% of the minerals, is also a partially weathered primary mineral. It is present within the profile, but also occurs in the surface horizons (Table 1).

**Table 2.** Major, trace and rare earth elements contents and weathering indices in soil phases

Elements	Horizon Sample	C (176 - 250 cm)		BC (126 - 176cm)			B (26 - 126cm)		A (0 - 26cm)
		R KR	KC	KBC3	KBC2	KBC1	KB2	KB1	KA
SiO <sub>2</sub>	Major elements in % of oxides	54.7	40.8	38.7	43.2	40.9	40.1	37.2	41.1
Al <sub>2</sub> O <sub>3</sub>		15.8	16.8	21.4	22.6	23.7	23.3	18.6	18.3
Fe <sub>2</sub> O <sub>3</sub>		8.1	14.4	14.4	10.1	10.2	9.9	15.9	12.5
TiO <sub>2</sub>		1.3	1.7	1.5	1.4	1.7	1.7	3.0	2.7
CaO		7.0	1.4	0.2	0.2	0.2	0.2	0.1	0.4
MgO		4.6	6.9	1.2	1.5	1.1	1.1	1.0	1.4
K <sub>2</sub> O		4.0	4.2	2.5	3.2	2.2	2.1	1.5	3.0
Na <sub>2</sub> O		3.1	0.4	0.1	0.1	0.1	0.1	0.1	0.3
SiO <sub>2</sub> /Al <sub>2</sub> O <sub>3</sub>	Weathering index %	2.9	2.1	1.5	1.6	1.5	1.5	1.7	1.9
Bases/R <sub>2</sub> O <sub>3</sub>		99.5	56.5	14.6	19.1	13.2	13.1	10.3	21.1
CIA		52.7	70.9	77.9	78.8	79.6	75.4	79.3	73.4
Ba	Traces elements in ppm	2706.0	3309.0	1197.7	1251.7	241.3	859.9	729.2	1700.2
Co		34.0	47.6	22.0	45.3	14.1	17.8	174.4	43.7
Cr		18.0	1133.0	299.0	213.0	610.0	264.0	381.0	339.0
Cu		6.0	26.9	33.9	28.9	38.1	31.9	53.4	38.0
Ga		24.0	28.2	24.9	24.8	30.4	31.8	26.9	26.2
Hf		1.0	2.5	2.6	2.3	4.6	3.4	6.2	5.3
Nb		9.0	10.8	16.6	14.4	35.2	20.7	35.5	30.4
Ni		116.0	227.9	48.7	53.6	70.8	61.9	81.9	65.4
Pb		20.0	20.1	26.4	23.0	21.1	24.9	28.4	25.4
Rb		83.0	102.7	27.9	20.5	21.2	16.5	40.8	27.5
Sn		1.8	7.9	2.0	1.9	2.5	3.0	4.1	3.8
Sr		1602.0	428.1	310.4	240.0	84.2	191.1	181.8	355.7
Ta		0.6	0.6	1.0	0.9	2.9	1.3	2.6	1.9
Th		3.1	3.7	6.1	3.2	9.2	5.5	9.9	6.1
Tl		0.4	0.5	0.4	0.5	0.2	0.4	1.1	0.5
U		0.8	0.9	1.9	1.3	2.9	1.8	2.8	1.8
V		122.0	247.0	367.0	255.0	638.0	273.0	455.0	361.0
W		0.5	0.4	0.8	0.6	1.2	0.9	1.4	1.1
Y		23.0	16.3	16.9	13.2	12.9	10.7	15.1	11.3
Zn		125.0	139.0	74.0	79.0	75.0	83.0	116.0	106.0
Zr	105.0	86.0	87.0	79.0	171.0	121.0	238.0	210.0	
La	Rare earth elements in ppm	52.7	38.7	42.6	10.8	61.6	14.7	57.4	32.9
Ce		85.9	94.4	105.2	31.6	111.6	34.1	163.9	72.8
Pr		10.9	11.0	13.8	4.0	15.9	4.9	14.2	9.1
Nd		46.8	45.3	58.6	17.9	59.1	20.6	51.9	35.4
Sm		9.1	7.9	1.9	4.1	2.5	4.4	4.1	6.4
Eu		4.0	2.1	2.9	1.1	2.1	1.2	1.9	1.7
Gd		8.1	5.5	8.3	3.6	5.4	3.6	5.3	4.4
Tb		0.9	0.7	1.1	0.5	0.6	0.5	0.7	0.5
Dy		3.9	3.8	5.7	2.8	3.6	2.9	3.8	3.1
Ho		0.7	0.6	0.9	0.5	0.5	0.5	0.6	0.5
Er		1.8	1.7	2.1	1.5	1.4	1.3	1.6	1.3
Tm		0.3	0.2	0.2	0.2	0.1	0.1	0.2	0.1
Yb		1.5	1.5	1.5	1.2	1.2	1.1	1.5	1.1
Lu		0.3	0.2	0.1	0.1	0.1	0.1	0.2	0.1
ΣREE	The REE Index	226.9	213.6	307.3	79.9	244.9	90.0	265.7	169.4
ΣLREE		209.4	199.4	293.4	69.5	225.0	79.9	252.8	158.3
ΣHREE		17.5	14.2	13.9	10.4	19.9	10.1	12.9	11.1
a		12.0	14.0	21.1	6.7	11.3	7.9	19.6	14.3
Ce/Ce*		1.0	1.3	1.6	1.3	1.2	1.1	1.0	1.2
Eu/Eu*		1.0	0.5	0.6	0.3	1.6	0.3	0.8	0.4
(La/Yb) <sub>N</sub>		1.0	0.7	1.1	0.3	0.8	0.4	1.5	0.9

a: ΣLREE/ ΣHREE

### Chemical elemental contents, mobilization and redistribution in various soil phases

#### Major and trace elements contents

Major and trace elemental contents and some weathering

indices are given in Table 2.

Silica (SiO<sub>2</sub>: 37.2 to 43.9%), aluminum (Al<sub>2</sub>O<sub>3</sub>: 16.8 to 23.7%) and iron (Fe<sub>2</sub>O<sub>3</sub>: 9.9 to 15.9%) are the most abundant elements in the soil phases. Silica contents decrease significantly from fresh rock to the dark grey soil matrix of the B horizon (SiO<sub>2</sub>: 54.7 to 37.2%), and slightly

**Table 3.** Enrichment factors (EF) for major and trace elements in various soil phases

	R	C	BC			B		A
		(176 - 250cm)	(126 - 176cm)		(26 - 126cm)		(0 - 26cm)	
	KR	KC	KBC3	KBC2	KBC1	KB2	KB1	KA
SiO <sub>2</sub>	1.0	0.6	0.6	0.7	0.6	0.6	0.3	0.4
Al <sub>2</sub> O <sub>3</sub>	1.0	0.8	1.2	1.3	1.1	1.1	0.5	0.6
Fe <sub>2</sub> O <sub>3</sub>	1.0	1.4	1.5	1.2	1.0	0.9	0.9	0.7
CaO	1.0	0.2	0.0	0.0	0.0	0.0	0.0	0.0
MgO	1.0	1.1	0.2	0.3	0.2	0.2	0.1	0.1
K <sub>2</sub> O	1.0	0.8	0.5	0.7	0.4	0.4	0.2	0.4
Na <sub>2</sub> O	1.0	0.1	0.0	0.0	0.0	0.0	0.0	0.0
Ba	1.0	0.9	0.4	0.4	0.1	0.2	0.1	0.3
Co	1.0	1.1	0.6	1.2	0.3	0.4	2.2	0.6
Cr	1.0	48.1	14.4	11.0	25.9	11.2	9.2	9.1
Cu	1.0	3.4	4.9	4.5	4.9	4.1	3.9	3.0
Ga	1.0	0.9	0.9	1.0	1.0	1.0	0.5	0.5
Hf	1.0	1.9	2.3	2.1	3.5	2.6	2.7	2.6
Nb	1.0	0.9	1.6	1.5	3.0	1.8	1.7	1.6
Ni	1.0	1.5	0.4	0.4	0.5	0.4	0.3	0.3
Pb	1.0	0.8	1.1	1.1	0.8	1.0	0.6	0.6
Rb	1.0	0.9	0.3	0.2	0.2	0.2	0.2	0.2
Sn	1.0	3.4	1.0	1.0	1.1	1.3	1.0	1.0
Sr	1.0	0.2	0.2	0.1	0.0	0.1	0.0	0.1
Ta	1.0	0.8	1.4	1.4	3.7	1.7	1.9	1.5
Th	1.0	0.9	1.7	1.0	2.3	1.4	1.4	0.9
Tl	1.0	1.0	0.9	1.2	0.4	0.8	1.2	0.6
U	1.0	0.9	2.1	1.5	2.8	1.7	1.5	1.1
V	1.0	1.5	2.6	1.9	4.0	1.7	1.6	1.4
W	1.0	0.6	1.4	1.1	1.8	1.4	1.2	1.1
Y	1.0	0.5	0.6	0.5	0.4	0.4	0.3	0.2
Zn	1.0	0.9	0.5	0.6	0.5	0.5	0.4	0.4
Zr	1.0	0.6	0.7	0.7	1.2	0.9	1.0	1.0

increase up to 41.1% at the soil surface. Inversely, aluminum (Al<sub>2</sub>O<sub>3</sub>: 15.8 to 23.7%) and iron (Fe<sub>2</sub>O<sub>3</sub>: 8.1 to 15.9%) contents increase invariably upwards. Calcium (CaO: 7.0 to 0.1%) and sodium (Na<sub>2</sub>O: 3.1 to 0.0%) are almost completely leached from all soil phases. However, potassium (K<sub>2</sub>O: 1.5 - 4.2%) and magnesium (MgO: 1.0 - 6.9%) contents remain relatively high, generally with increasing values from fresh rock to the pink saprolite (K<sub>2</sub>O: 4.0 to 4.2%; MgO: 4.6 to 6.9%). The molar ratio SiO<sub>2</sub>/Al<sub>2</sub>O<sub>3</sub>, related to silica leaching intensity, remains relatively high in all the soil phases (1.5 to 2.1), and decreases slightly towards the surface. The chemical index of alteration (CIA), related to weathering intensity, increases very slightly from the pink saprolite towards the surface horizons (CIA: 70.9 to 79.6%). Furthermore, the bases/R<sub>2</sub>O<sub>3</sub> ratio, giving an estimation of the weatherable primary minerals remaining in soils, decreases moderately upwards from the pink saprolite (56.5%) through the reddish brown saprolite to 10.3% in the dark grey soil matrix.

The most abundant trace element in this weathering mantle is Ba (3309.0 ppm in the pink saprolite), followed

by Cr (1133.0 ppm), V (638.0 ppm), Sr (428.1 ppm), Zr (238.0 ppm), Ni (227.9 ppm), Co (174.4 ppm), Zn (139.0 ppm) and Rb (102.7 ppm) in various soil phases (Table 2). Overall, trace elements in this weathering mantle can be grouped into three main categories according to their behavior in the soil phases compared to the fresh rock. They are: elements with increasing contents in soil phases (Cr, V, Cu, Nb, Ta, Th, Hf, Pb, Sn, U and W); elements with decreasing contents in soil phases (Sr and Y); and elements with alternately increasing and decreasing contents in soil phases (Ba, Co, Ga, Ni, Rb, Tl, Zn and Zr).

### Major and trace elements balance

Enrichment-depletion of major and trace elements in this weathering mantle was assessed using enrichment factors (EF). These results are presented in Table 3.

Major and trace elements in various soil phases are grouped into enriched (EF ≥ 1.0), depleted (EF < 1.0) or alternately enriched-depleted (EF ± 1.0) elements (Table

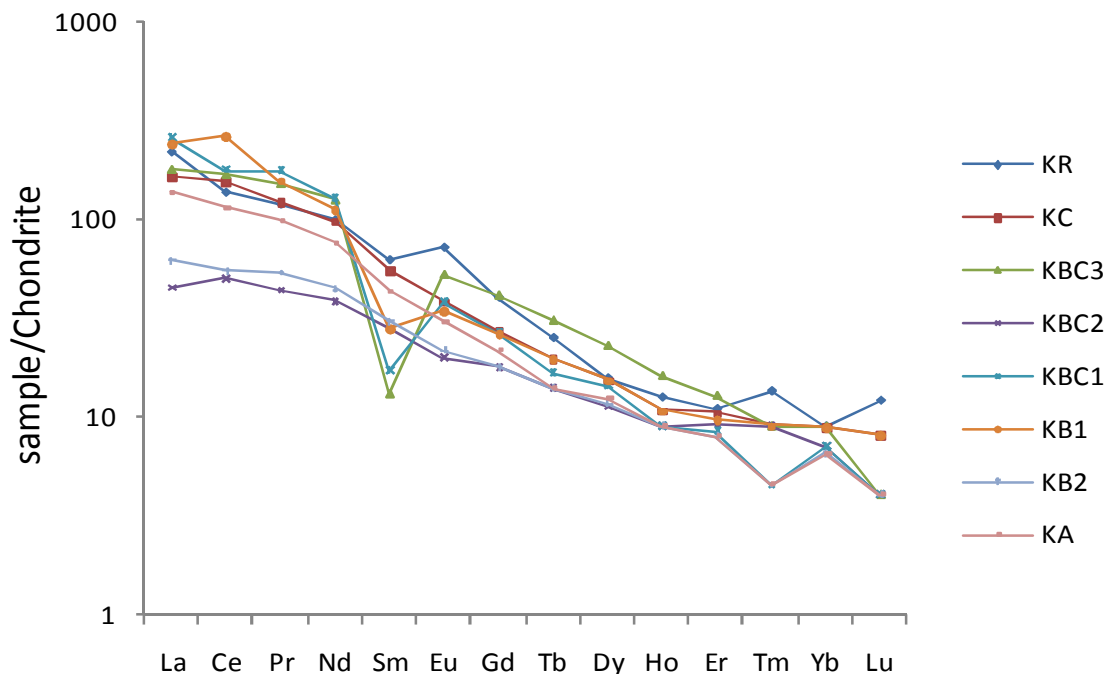


Figure 4. CI Chondrite-normalized REE patterns for various soil phases

3). Enriched elements are Cr, Cu, V, Hf and Sn. They are enriched in all the soil phases. Cr is the most enriched, with EF between 9.1 and 48.1; followed by Cu (EF: 3.0 to 4.9); V (EF: 1.4 to 4.0), Hf (EF: 1.9 to 3.5) and Sn (EF: 1.0 to 3.4). The highest enrichments of V and Hf are in the yellow brown soil matrix (EF<sub>V</sub>: 4.0; EF<sub>Hf</sub>: 3.5); those for Cu and Sn are in the reddish brown saprolite and in the yellow brown soil matrix Cu (EF<sub>Cu</sub>: 4.9) and the pink saprolite Sn (EF<sub>Sn</sub>: 3.4). Depleted elements include Si, Ca, K, Na, Ba, Ga, Rb, Sr, Y and Zn. They are strongly depleted, with EF ≤ 0.2 like in Ca, Na and Sr, or slightly depleted, with EF ranging from 0.5 to 0.9 like in Si, K, Ba, Ga, Rb, Y and Zn. Thus, in all the soil phases of the Kékem weathering mantle, Ca, Na and Sr are almost completely leached, whereas Si, K, Ba, Rb, Y and Zn are increasingly depleted towards the soil surface, and Ga remains very slightly depleted. Alternately enriched and depleted elements include Al, Fe, Mg, Co, Nb, Ni, Pb, Ta, Th, Ti, U, W and Zr. Elements such as Nb, Ta, U and W are very slightly depleted in the pink saprolite, but enriched in the other soil phases. Al, Pb, Co, Zr and Ti are invariably depleted and enriched, with EF<sub>Al</sub>: 0.5 to 1.3; EF<sub>Pb</sub>: 0.6 to 1.1; EF<sub>Co</sub>: 0.3 to 2.2; EF<sub>Zr</sub>: 0.6 to 1.2 and EF<sub>Ti</sub>: 0.4 to 1.2. Th is slightly depleted in the pink saprolite and the dark brown soil matrix (EF: 0.9), but enriched in the other soil phases (EF: 1.0 to 2.3). Fe, Mg and Ni are enriched in the subsoil, and depleted in the surface horizons.

### The REE elements

In the Kékem weathering mantle, abundance of the REE varies from  $\sum$ REE: 79 ppm in the whitish grey soil matrix to 307.3 ppm in the reddish brown saprolite (Tab. 2). In general, the REE in various soil phases are more enriched compared to the BSE (Mc Donough and Sun, 1995), with enrichment rates (ER) ranging from 11.5 to 44.8. The LREE are the most abundant, with  $\sum$ LREE ranging from 69.5 to 293.4 ppm. The most abundant LREE is Ce (163.9 ppm in the dark grey soil matrix), followed by La and Nd (with values of 61.6 ppm and 59.1 ppm respectively in the yellow brown soil matrix). Concentrations of the HREE did not exceed  $\sum$ HREE: 20 ppm.

The REE fractionation index,  $a: \sum$ LREE/ $\sum$ HREE, which ranges from 6.7 to 21.1, highlights important accumulations of the LREE in the soil phases. The highest accumulations are in the reddish brown saprolite ( $a$ : 21.1) and the dark grey soil matrix ( $a$ : 19.6). The Eu/Eu\* ratio, related to the REE fractionation, varies from 0.9 to 2.3, indicating important fractionation of the REE in various soil phases, with significant Eu anomaly. The Ce/Ce\* ratio, ranging from 0.8 to 1.4, points out to a positive anomaly of Ce, except in the yellow brown and the pale red soil matrices (Tab. 2). The (La/Yb)<sub>N</sub> ratio, which ranges from 6.3 to 36.1, also indicates a strong fractionation of the LREE compared to the HREE.

The Chondrite-normalized REE patterns illustrated in Figure 4 confirm the marked fractionation of the REE in

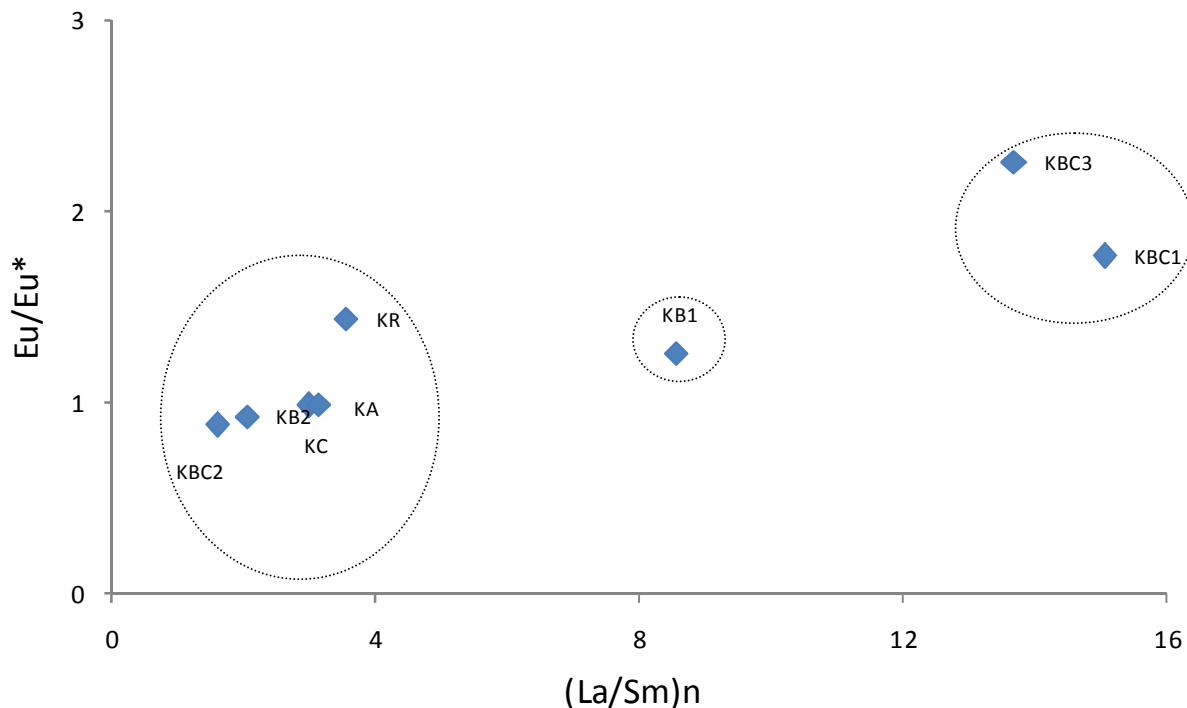


**Figure 5.** Variation of Eu anomaly versus LREE fractionation in various soil phases

all the soil phases, from La to Dy. This REE fractionation in soil phases is not very significant from Ho to Lu. These Chondrite-normalized REE patterns, as well as the variability of the  $Eu/Eu^*$  as a function of the  $(La/Sm)_N$  (Figure 5), makes it possible to classify soil phases in this weathering mantle into three main categories: (i) soil phases with slightly pronounced LREE fractionation and Eu anomaly represented by the pink saprolite, and the whitish grey, the pale red and the dark brown soil matrices; (ii) soil phases with strong LREE fractionation and slightly pronounced Eu anomaly such as the dark grey soil matrix; and (iii) soil phases with very strong LREE fractionation and Eu anomaly like the reddish brown saprolite and the yellow brown soil matrix. The norite-normalized REE patterns (not shown) also reveal a significant fractionation of the REE compared to the fresh rock, with the pink and the reddish brown saprolites, the yellow brown and the dark grey soil matrices relatively enriched in LREE.

## DISCUSSION

### Weathering trends and intensity in the Kekem weathering mantle

In the Kekem weathering mantle, the pink and the reddish brown saprolites have preserved the medium-grainy structure of norites that is indicated by the

presence of the crystal-rich plasma as well as micrometric and polychromatic punctuations. Chemical weathering with conservation of the rock structure is evenly reported in tropical regions (Nguetnkam *et al.*, 2003; Nahon and Merino, 1997; Yongue-Fouateu, 1986; Delvigne, 1965). It has usually contributed to generation of the saprolites (Nahon, 1991). Moreover, the weathering of norites in Kekem has led to the formation of 2:1 clay minerals (sepiolite and smectite) as well as relatively low leaching of Si, Mg and K to lower soil depths. Presence of these 2:1 clay minerals, with recurrence of mineral springs and low exportation of Si, Mg and K in these environments are indicative of a highly confined alkaline milieu suitable for specific hydrolysis known as bisiallisation (Nguetnkam *et al.*, 2003). The relatively low values of CIA (70.9 – 79.6%) in soil phases of the Kekem weathering mantle suggest a restrained weathering process in this environment that led to the formation of 2:1 clay minerals. Additionally, in this weathering mantle, the high  $SiO_2/Al_2O_3$  molar ratio (1.5 to 2.1) reinforces the presence of 2:1 clay minerals and relatively low leaching of silica in this environment. Also, the relatively high values of bases/ $R_2O_3$  in various soil phases (10.3 – 56.5%) highlight limited leaching of the alkali cations (Little and Aeolus, 2006), more specifically Mg and K. This can be attributed to sepiolite and smectite development that need important consumption of Mg and K respectively (Kadir *et al.*, 2002). Limited exportation of the alkali cations from the topsoil could be related to

persistence of rock fragments (Tematio *et al.*, 2009). All these statements indicate that the Kekem weathering mantle has experienced restrained weathering process with minor pedological differentiation.

### Occurrence of specific secondary minerals

The mineral data of the Kekem weathering mantle have revealed the presence of unusual minerals like sepiolite, akaganéite and berthierine.

Sepiolite is a Mg hydrated silicate with general formula  $[\text{Mg}_4\text{Si}_6\text{O}_{15}(\text{OH})_2 \cdot 6\text{H}_2\text{O}]$ . It is a poorly crystallized 2:1 clay mineral with a fibrous structure (Kadir *et al.*, 2002). Nickel (Ni), Mn, Fe and Al are the main impurities (Caillère *et al.*, 2004) and may replace Mg in the crystal lattice or associated with  $\text{H}_2\text{O}$  in the channels of the mineral structure (Kadir *et al.*, 2002). Sepiolite is commonly found in weathering products in saline or alkaline environments (Kadir *et al.*, 2002; Singer *et al.*, 1998). But, the configuration of the Kekem area makes it a highly confined alkaline milieu. For instance, the poor drainage in this environment may result to the collapsing lowland structure of this area which belongs to the *Mbô* plain. Its alkaline status may be attributed to mineral springs. Under these alkaline conditions, released Si and Mg may have served in the formation of sepiolite during precipitation under highly confined conditions (McLean *et al.*, 1972).

Akaganéite is an iron oxide-hydroxide/chloride mineral  $[\beta\text{-Fe}^{3+}\text{O}(\text{OH},\text{Cl})]$  with tunnel structure, sheaflike morphology with Ni as impurity (Xiong *et al.*, 2008). It has attracted much investigation because of its sorption, ion exchange and catalytic properties (Fitzpatrick and Shand, 2008). It has since been recognized as a Fe-oxide component rarely observed in soils. Nevertheless, the highly alkaline environment provides ideal conditions for its crystallization in soils (Bibi *et al.*, 2011). In the Kekem weathering mantle, akaganéite has been identified as a significant weathering product in the soil phases (16 to 75% of minerals detected by X-ray). In these highly confined alkaline conditions, it apparently forms from dissolution of pyroxene with release of free  $\text{Fe}^{2+}$ . Under exposure in alternately humid and dry conditions during a long period of time, free  $\text{Fe}^{2+}$  can be oxidized, leading to the formation of akaganéite (Garcia *et al.*, 2008; Bigham *et al.*, 2002).

Berthierine is a tri-octahedral Fe-rich clay mineral with the general formula  $[(\text{Fe}^{2+}, \text{Fe}^{3+}, \text{Mg}, \text{Al})_{2-3}(\text{Si}, \text{Al})_2\text{O}_5(\text{OH})_4]$ . It has a 1:1 type structure, and is related to the serpentine subgroup of clay minerals. It contains a greater range of minor and trace elements substitution. Berthierine has been very little reported in soils (Kodama and Foscolos, 1981). However, some workers suggested that berthierines in soils may have formed in poorly oxygenated conditions during pedogenesis or

hydrothermal alteration (Moore and Hughes, 2000). In the Kekem weathering mantle, berthierines occur in all the soil phases. Thus, in the Kekem area which is like a highly confined alkaline environment, berthierine may probably have formed through the dissolution of feldspars in the presence of Fe-rich solution (Wise, 2007).

### Occurrence of rare metals

In the Kekem weathering mantle, medium grade accumulation of Ba (241.0 to 3309.0 ppm), Cr (213.0 to 1133.0 ppm), V (247.0 to 638.0 ppm) and Sr (84.2 to 428.1 ppm) have been observed. Other rare metals like Zr (121.0 to 238.0 ppm), Ni (227.9 ppm), Co (174.4 ppm), Zn (106.0 to 139.0 ppm) and Rb (102.7 ppm) also exhibit significant accumulations in specific soil phases. The mass balance evaluation reveals that Cr, Cu, Hf, V, Nb, Ta, U and W considerably accumulate in soil phases. The rare metals accumulations in weathering mantles originated from the alteration of basic rocks are well known around the world (Singh *et al.*, 2012; Ames and Farrow, 2007; Moyen, 2007). In the Kekem weathering mantle, it could have resulted from relative enrichment during hydrolysis in association with Fe-oxides (Singh *et al.*, 2002) during which rare metals accumulate due to poor drainage of the percolating groundwater (Yongue-Fouateu *et al.*, 2006). It may also resulted from slow and partial dissolution of the neosynthesis of secondary minerals through weathering (Singh *et al.*, 2002) or incorporation into relatively resistant primary minerals such as Cr-rich magnetite, rutile, apatite, phlogopite and zircon (Lowson *et al.*, 1986). It could lastly be attributed to intense biological activity due to recycling process of metals by plants at the soil surface (Kabata-Pendias, 2001). Copper (Cu), Hf, Nb, Ta, U and W, despite their high enrichment rates, remain little concentrated in all the soil phases. This could be due to the very low concentrations of these rare metals in fresh norites.

In the Kekem weathering mantle, some other rare metals, despite their relative low contents, remain of great interest. They are Pb, Y, La, Ce, and Nd. Their relative low concentrations in soil phases suggest that they may either remain incorporated in more resistant primary minerals and residual heavy minerals (Lowson *et al.*, 1986); or are trapped during neosynthesis of secondary minerals (Singh *et al.*, 2002), or may be taken up through recycling process of metals by plants (Kabata-Pendias, 2001). In addition, the LREE accumulation in soil phases as illustrated by high  $(\text{La}/\text{Yb})_N$  values (6.3 – 36.1) may be attributed to intense REE fractionation (Moroni *et al.*, 2001). Thus, concentration of REE in soil phases highlights the influence of secondary minerals development on the REE redistribution during the weathering process. Moreover, the strong positive Ce anomaly may be linked to oxidation of  $\text{Ce}^{3+}$  to  $\text{Ce}^{4+}$  or

primary  $Ce^{4+}$  in residual zircon minerals because of its oxidation ability, insolubility and stability in lateritic environments (Ndjigui *et al.*, 2008).

## CONCLUSION

This paper focused on the occurrence of sepiolite, akaganéite and berthierine, and medium grade accumulation of rare metals in the Kekem norites weathering mantle. Macroscopic and microscopic organization of various soil phases in this weathering mantle as well as their mineral composition and chemical elements mobilization and redistribution enable us to draw the following conclusion:

- This weathering mantle has been subjected to restrained weathering process with minor pedological differentiation;
- The major weathering process in this area, referred to as bisiallisation, led to formation of 2:1 clay minerals such as sepiolite and smectite;
- The highly confined alkaline conditions prevailing in this area have contributed to the formation of unusual secondary minerals like sepiolite, akaganéite and berthierine in these soils;
- Accumulation of rare metals, more specifically Ba, Cr, Sr, Zr, Ni, Co, Zn and Rb, and to some extent Cu, Hf, Sn, Nb, Ta, Th, U and W, in this weathering mantle could have resulted from: (i) relative enrichment during hydrolysis of weatherable primary minerals, (ii) slow dissolution of the neosynthesis secondary minerals or relatively resistant primary minerals, (iii) intense biological activity with recycling of metals by plants at the soil surface;
- There is a strong REE fractionation in various soil phases of this weathering mantle from La to Dy, with high Eu anomaly.

Overall, the Kekem norites weathering mantle may be compared to a potential deposit with its relatively high accumulation of sepiolite, akaganéite and berthierine, and medium grade concentrations of rare metals (mainly Ba, Cr, Sr and V) in soil phases.

## REFERENCES

- Ames DE, Farrow CEG (2007). Metallogeny of the Sudbury mining camp, Ontario, in Goodfellow, W.D., ed., Mineral Deposits of Canada: A Synthesis of Major Deposit-Types, District Metallogeny, the Evolution of Geological Provinces, and Exploration Methods: *Geological Association of Canada, Mineral Deposits Division, Special Publication*, 5, 329-350
- Anders E, Grevesse N (1989). Abundances of the elements: meteoritic and solar. *Geochimica and Cosmochimica Acta*, 53 (1), 197-214
- Bibi I, Singh B, Silvester E (2011). Akaganéite ( $\beta$ -FeOOH) precipitation in inland acid sulfate soils of south-western New South Wales (NSW), Australia. *Geochimica and Cosmochimica Acta*, 75, 6429–6438
- Bigham JM, Fitzpatrick RW, Schulze DG (2002). Iron oxides. p. 323-366. In *Soil mineralogy with environmental applications*. Edited by Dixon, J.B. and D.G. Schulze. Madison, WI: *Soil Sci. Soc. Am.*
- Birkeland PW (1999). Soils and Geomorphology. *Oxford University Press, New York*, pp 430
- Caillère, S, Hénin S, Rautureau M (2004). Les Argiles. *Paris, Éditions Septima*
- Delvigne J (19650). Pédogenèse en zone tropicale. La formation des minéraux secondaires en milieu ferrallitique. *Mémoire ORSTOM*, 13, pp177
- Déruelle B, Moreau C, Kambou R, Lisson, jonfang E, Ghogomu RT, Nono A (1991). The Cameroon Line : a review. In *Magmatism in Extensional Structural Settings*. A.B. Kampuzu et R.T. Lubala Eds, *Springer-Verlag*, 274-327
- Fitzpatrick R, Shand P (2008). Inland acid sulfate soils: overview and conceptual models. In *Inland Acid Sulfate Soil Systems Across Australia* (Eds. R. Fitzpatrick and P. Shand), 6-74
- Garcia KE, Barrero CA, Morales AL, Greneche JM (2008). Characterization of akaganéite synthesized in presence of  $Al^{3+}$ ,  $Cr^{3+}$ , and  $Cu^{2+}$  ions and urea. *Materials Chemistry and Physics*, 112, 120–126
- Hamman JN, Rozendaal A, Jordaan W (1996). Gabbro-norite hosted Ni-Cu-(Co)-Sulfide mineralization in Southern Namaqualand and its relationship to the cupriferous Koperberg Suite of the Okiep Copper District, South Africa. *South Afr. J. Geol.* 99 (2), 153-167
- Kabata-Pendias A (2001). Traces Elements in Soils and Plants. *3<sup>rd</sup> Ed. CRC Press LLC, USA*, pp. 413
- Kadir S, Bas H, Karakas Z (2002). Origin of sepiolite and loughlinitite in a neogene volcano-sedimentary lacustrine environment, Mihaliççik-Eskisehir, Turkey. *The Canadian Mineralogist*, 40, 1091-1102
- Kodama H, Foscolos AE (1981). Occurrence of berthierine in Canadian arctic desert soils. *The Canadian Mineralogist*, 19, 279-283
- Kwékam M (2005). Genèse et évolution des granitoïdes calco-alkalins au cours de la tectonique panafricaine: le cas des massifs syn- à tardi-tectoniques de l'Ouest-Cameroun (Régions de Dschang et de Kekem). *Thèse Doctorat Etat, Université de Yaoundé I*, pp 194
- Kwékam M, Liégeois JP, Njonfang E, Affaton P, Hartmann G, Tchoua F (2010). Nature, origin and significance of the Fomopéa Pan-African high-K calc-alkaline plutonic complex in the Central African fold belt (Cameroon). *J. Afr. Earth Science*, 57, 79–95
- Lee C (1996). A review of mineralization in the Bushveld Complex and some other layered mafic intrusions. In: layered intrusions. R.G. Cawthorn Ed., *Elsevier, Amsterdam*, 103-146
- Little MG, Aeolus LCT (2006). On the formation of an inverted weathering profile on Mount Kilimanjaro, Tanzania: Buried paleosol or groundwater weathering. *Chemical Geology*, 235, 205–221
- Lowson RT, Short DA, Davey BG, Gray DJ (1986).  $^{238}U/^{235}U$  and  $^{230}Th/^{234}Th$  activity ratios in minerals phases of alteritic weathered zone. *Geochimica and Cosmochimica Acta*, 50, 1697-1702
- Mc Donough, WF, Sun SS (1995). The composition of the Earth. *Chemical Geology*, 120, 223-253
- McLean SA, Allen BL, Craig JR (1972). The occurrence of sepiolite and attapulgite on the southern High plains. *Clay and Clay Minerals*, 20, 143-149
- McLennan SM (1989). Rare earth elements in sedimentary rocks: influence of provenance and sedimentary processes. In: Lipin, B.R., McKay, G.A. Ed., *Geochemistry and Mineralogy of Rare Earth Elements*. *Review Mineralogy*, 21, 169–196
- Moore DM, Hughes RE (2000). Ordovician and pennsylvanian berthierine-bearing flint clays. *Clays and Clay Minerals*, 48 (1), 145-149
- Moroni M, Girardi VAV, Ferrario A (2001). The Serra Pelada Au-PGE deposit, Serra dos Carajas (Para State, Brazil): geological and geochemical indications for a composite mineralising process. *Mineral Deposita*, 36, 768–785
- Moyen JF (2007). Le complexe de Bushveld. *Livret-guide excursion Association meta-odos Février 2007*, pp34
- Nahon D (1991). Introduction to the petrology of soils and chemical weathering. *John Wiley and Sons Ed., New York*, pp297
- Nahon D, Merino E (1997). Pseudomorphic replacement in tropical

- weathering: evidence, geochemical consequences and kinetic-rheological origin. *American Journal of Science*, 297, 393–417
- Ndjigui PD, Bilong P, Bitom D, Dia A (2008). Mobilization and redistribution of major and trace elements in two weathering profiles developed on serpentinites in the Lomié ultramafic complex, South-East Cameroon. *Journal of African Earth Science*, 50, 305–328
- Nestbitt HW, Young GM (1989). Formation and diagenesis of weathering profiles. *J. Geol.* 97, 129-147
- Nguetnkam JP, Bitom D, Yongue R, Bilong P, Belinga ESM, Volkoff B (2003). Etude pétrologique, minéralogique et géochimique d'une toposéquence de sols développés sur granite dans le plateau forestier Sud-Camerounais. *Sciences, Technique et Développement*, 10, 35-43
- Rahn KA, Mc Cafrey RJ (1979). Compositional differences between Arctic aerosol and snow. *Nature*, 280, 479–480
- Ruxton BP (1968). Measures of the degree of chemical weathering of rocks. *J. Geol.* 76, 518–527
- Singer A, Stahr K, Zarei M (1998). Characteristics and origin of sepiolite (Meershaum) from central Somalia. *Clay Minerals*, 33, 349-362
- Singh B, Sherman DM, Gilkes RJ, Wells MA, Mosselmans JFW (2002). Incorporation of Cr, Mn and Ni into goethite ( $\alpha$ -FeOOH): mechanism from extended X-ray absorption fine structure spectroscopy. *Clay Minerals*, 37, 639–649
- Singh H, Jotisankasa A, Huat BBK (2012). Residual soils of Southeast Asia. In *Hanbook of Tropical Residual Soils Engineering*. G. David and B.B.K. Huat Ed., 491-532
- Taylor, S.R., McLennan, S.M., 1985. The Continental Crust: its Composition and Evolution. *Blackwell, Oxford*, pp 312
- Tematio P, Fritsch E, Hodson ME, Lucas Y, Bitom D, Bilong P (2009). Mineral and geochemical characterization of a leptic aluandic soil and a thapto aluandic-ferralsol developed on trachytes in Mount Bambouto (Cameroon volcanic line). *Geoderma*, 152, 314-323
- Wise MA (2007). Crystallization of 'pocket' berthierine from the pulsifer granitic pegmatite, Poland, Maine, USA. *The Clay Minerals Society*
- Xiong H, Liao Y, Zhou L (2008). Influence of chloride and sulfate on formation of akaganéite and schwertmannite through ferrous biooxidation by *Acidithiobacillus ferrooxidans* cells. *Environmental Science and Technology*, 42(23):8681-6
- Yongue-Fouateu R (1986). Contribution à l'étude pétrologique de l'altération et des faciès de cuirassement ferrugineux des gneiss migmatitiques de la région de Yaoundé. *Thèse 3e cycle, Université de Yaoundé*, pp214
- Yongue-Fouateu R (1995). Les concentrations métallifères de nickel et de cobalt à partir de l'altération latéritique des roches ultrabasiqes serpentinisées du Sud-Est Cameroun. *Thèse Doctorat ès. Sciences, Université de Yaoundé I*, pp262
- Yongue-Fouateu R, Ghogomu RT, Penaye J, Ekodeck GE, Stendal H, Colin F (2006). Nickel and cobalt distribution in the laterites of the Lomié region, South-East Cameroon. *J. Afr. Earth Sci.* 45, 33–47